

RESEARCH

Open Access



Hygromechanical behaviour of wooden panel paintings: classification of their deformation tendencies based on numerical modelling and experimental results

Lorenzo Riparbelli¹, Paola Mazzanti^{1*}, Chiara Manfriani¹, Luca Uzielli¹, Ciro Castelli², Giovanni Gualdani^{1,2}, Luciano Ricciardi², Andrea Santacesaria², Sandra Rossi² and Marco Fioravanti¹

Abstract

Wooden panel paintings are among the most important historical and artistic artworks from the Middle Ages and the Renaissance period. Currently, they represent a challenge for conservators and scientists who face complex issues related to their conservation. Panel paintings can be considered multilayer objects, that for brevity can be considered to consist of a wooden support and various paint layers. The wooden support is known to be hygroscopic and is continuously seeking hygroscopic equilibrium with the humidity of the environment, thus it tends to deform. Based on various hygroscopic tests carried out on 6 real panel paintings chosen by expert restorers to represent different periods and construction techniques, this paper describes the deformation tendencies of the selected panel paintings. Among possible variables, three most important variables were identified: (a) tree ring orientation of the wooden support, (b) stiffness and (c) emissivity of the paint layers. The internal equilibrium of the forces, governed by the moisture gradients across the thickness of the wood, changes drastically according to the varying characterisation of these factors. To observe their individual contributions, the 6 panel paintings underwent various humidity cycles, were completely free to deform and were always in complete safety. To characterise the stiffness and emissivity of the paint layers, the 6 panel paintings underwent a few humidity cycles with the front face totally waterproofed; thus, the moisture exchange was forced from the back only, and one of the three variables was eliminated. A complex system emerges where the tree ring orientation of the wooden support, the stiffness and emissivity of the paint layers are strongly coupled and determine the deformation modes of the panel paintings. A numerical analysis was conducted to classify the various general deformation modes of panel paintings and the specific classification of the 6 real panel paintings analysed experimentally. The complexity of the interaction of the variables studied suggests that experimental procedures must be conducted in preparation for numerical analyses of real panel paintings.

Keywords Wooden panel paintings, Conservation, Experimental tests, Numerical modelling, Panel painting deformation tendencies, Paint layer emissivity, Paint layer stiffness

Introduction

Wooden panel paintings (WPPs) are some of the most valuable cultural heritage artworks. In recent decades, WPP preservation has been the object of several scientific studies [1–5], that have attempted to solve critical questions such as those concerning their interaction with conservation environments.

*Correspondence:

Paola Mazzanti
paola.mazzanti@unifi.it

¹ DAGRI, University of Florence, Florence, Italy

² Opificio delle Pietre Dure, Florence, Italy

WPPs have a multilayered structure schematically represented by wooden supports, often made of different boards covered on one side with paint layers (occasionally, the back of the panel was covered by a light coat, historically used to balance the moisture entering from both sides of the panel), and typically equipped on its back with a restraining system. The paint layers are constituted by a ground layer, mainly glue and gesso, sometimes canvas, pigments or dyes included in tempera or oil binders, and often by a varnish layer on top [6, 7]. The structural characteristics of WPPs, together with their construction techniques, have changed over time. In Italy, the period between the 12th and the first half of the fifteenth century was characterised by a wide production of large polyptychs and painted crosses. In this period, the ground layers were solid and strong, including the presence of canvas with a still-valid structural function, when the canvas covered the frame. Later, from the second half of the fifteenth century, characterised by altarpieces, the ground layers were lighter and thinner [8].

According to Cennini [9], the preparation of the panel began with several coats of animal glue to saturate the porosity of the wood. Several layers of ground, usually made of gesso and animal glue, were subsequently laid down. It is known that the ground layers may have different compositions—glass, kaolin, calcium carbonate, among others, were identified [10]—being in any case the thicker layer, measuring from 250 μm up to 1800 μm [11] without canvas. Canvas could be applied below ground layers to cushion the impact of the moisture-induced movements of the wood on the paint film. The presence of the canvas was discontinuous over time, becoming less common in the late fifteenth century. On top of the paint layers, the thinner varnish layer strongly contributes to defining the emissivity [12] of the artwork, because it is the most superficial layer and was made of low-hygroscopic materials, such mastic, and other natural resins in the past or resins such as aliphatic, acrylic and urea-aldehyde, among others, in the case of modern restoration resins [13–17]. By contrast, the other layers of the WPP structure are made of hygroscopic materials [1–3], primarily wood and ground layers, which may expand or shrink according to their own properties under climatic variations. Henceforth, for brevity, all these layers will be referred to collectively as the paint layers.

Due to this complex structure, the mechanical and hygroscopic properties of the constitutive materials are quite different; in the case of climatic variations, the shrinking/swelling tendencies contribute to generating inner stresses between the wooden support, the paint layers and at their interface [1, 2]. Moreover, when not properly dimensioned, the interaction between the wooden boards and the restraining system can worsen

the conservation conditions of the artworks [8] producing damage both on the paint layers [1, 8] and on the wooden support [1–3, 8], and/or irreversible deformations that determine the typical cupping that can be observed in many panel paintings [8].

Typically, deformations of panel paintings are induced by the variation of the relative humidity of the air (RH), and they can be either permanent or transitory [1, 18]. In addition, the mechanisms responsible for their origin have not yet been conclusively established, and some of those considered to be the most relevant most likely occur at the same time to determine the deformational behaviour of the paintings, as this paper attempts to demonstrate. For clarity, the most important causes are reported below according to deformation typology.

a) Permanent deformation

- Tree ring orientation: it is well-known that wood is an anisotropic material for which shrinkage and swelling are twice as high along the tangential direction compared to the radial direction [19]. Such behaviour causes a typical cupping of the tangential boards that also remains at the equilibrium state;
- Compression set: namely, the permanent deformation remaining after removal of a force. This is caused by repeated RH cycles that induce internal tension–compression stresses in the wooden support. When the RH varies, a change in the moisture content (MC) occurs, first in the most superficial layers of the exposed back of the boards that consequently produce dimensional changes. However, the inner wood layers that are not yet involved in such a process, do not yet shrink or swell, with the consequent internal stresses within the wood thickness causing permanent cupping of the panel [18, 20]. It is possible that a first manifestation of such a mechanism occurs with the preparation of the wooden support when a large amount of water is introduced in the panel by means of animal glue and gesso [21];
- Wood ageing: with time, wood loses hemicelluloses from the back surface of the wooden panel towards the inner layers, with a progressive reduction in the hygroscopicity of the surface layer compared to the inner layers [22, 23]. This mechanism can produce a 'moisture gradient' across the wood panel that over time can contribute to its permanent deformation;
- Panel's mechanical asymmetry: the back of the panel has the mechanical properties typical of the wooden species, whereas the front has mechanical properties heavily influenced by those of the paint layers (ground, paints, and varnish). In fact, wood and

paint layers show different hygromechanical properties [14, 15], with ground layers stiffer than wood in its transverse directions, and the paint layers due to their complexity and despite their small thickness can significantly affect the deformational behaviour of the whole panel. Their mechanical contribution to the permanent deformation must be taken into account [1, 21, 24];

b) Transient deformation In addition to permanent deformations, transient deformation can also occur as a consequence of RH variations. These variations arise from the hygroscopic asymmetry between the two faces of the panel painting, the bare wood on the back and the painted face on the front. This transient state is characterised by the onset of asymmetric moisture gradients across the panel thickness, that may produce a typical deformation known as flying wood [25, 26]. A note: [25] uses the term flying wood to describe the deformations of wooden boards with an asymmetric hygroscopicity with large mechanosorption effects; in the panel paintings conservation, the same term flying wood describe deformations where the mechanosorption effects can be considered negligible, and this is the meaning of the term used in this paper.

Within this theoretical framework, this paper presents the results from an experimental campaign carried out on six historic panel paintings. The WPPs, dated from the 15th to 16th century, were subjected to several cycles of controlled RH variations that were compatible with RH fluctuations already sustained by paintings (determined according to EN15757:2010 [27]) in the restoration environment, without any damage visible when analysed by restorers, and their actual time history of deflection was monitored. The experimental tests allowed us to establish the main mechanisms causing the deformations in the panel paintings, together with their specific contribution. In addition, a numerical model was developed and was able to interpret such behaviour and highlight the complexity of the phenomenon acting through the interaction of these mechanisms.

The aim of the research is to understand the deformation dynamics in a population of WPPs chosen by experienced restorers as representative of both different techniques and construction typologies relevant to the Italian school in the periods between the fifteenth and sixteenth centuries and to establish the existence of various deformation modes within the examined structural typologies.

The hygroscopic behaviour of wood is well described in the literature; however, the deformation tendencies of panel paintings are more complex because they are also

influenced by the interaction of the hygromechanical behaviour of the wooden support with the hygromechanical behaviour of the paint layers that may have a moisture barrier and mechanical stiffening behaviour. For the experimental validation, the present study assumes that the main variables influencing the actual deformation dynamics of WPPs are a) the stiffness of the wood and the paint layers, (b) the moisture diffusion of wood and emissivity of wood and paint layers, and (c) the tree ring orientation of the wooden panel. Thus, a numerical model was developed (a) to classify the hygromechanical behaviour of the panel paintings and (b) to explore how the complex interaction among these three variables affects such behaviour.

Materials and methods

Panel paintings and monitoring equipment

Six panel paintings were chosen for testing. Table 1 shows images (front and back) of the investigated paintings, along with the name, dimensions, age and painting technique specifications. They are labelled by 'WPP' followed by a progressive number, as follows: WPP1 corresponds to '*Madonna with Child*', WPP2 to '*Saint Lodovico and Saint Giuliano*', WPP3 to '*Dominican Saint*', WPP4 to '*Madonna with Child, Saint John and monk*', WPP5 corresponds to '*Crucifixion with Madonna and Saint John*', and WPP6 to '*Madonna with Child*'. These WPPs, whose wooden support is made of poplar wood (*Populus alba* L.), were chosen according to OPD (Opificio delle Pietre Dure, restoration laboratory in Florence, Italy) art conservators' observations; they are considered representative of historical changes (see "introduction" Section) during a time span between the fifteenth and sixteenth century for construction features, ground layer and painting/artistic technique, or conservation conditions.




Each panel painting was equipped with a Deformometric Kit (DK) to measure the deformation behaviour, the panel shrinking and swelling and, by means of data processing and trigonometrical calculations, the variations in cupping angle (ϕ , °) and deflection (δ_{\max} , mm) induced by climatic fluctuations [28]. The DKs geometric parameters are presented in Table 2. All sensors were connected to a Pace Scientific XR5-SE data logger (accuracy $\pm 0.25\%$) that powered the instruments and logged the data every 15 min. The collected data were elaborated through a customised data code.

To obtain a controlled and stable environment, an RH-controlled box (1.20 m \times 1.80 m \times 2.00 m, 4.32 m³ volume total) was constructed using a wooden frame and thermoinsulated panels. The temperature (T) was not controlled and depended on the controlled ambient conditions of the OPD Lab, and the small variations were

Table 1 Description of the six paintings and their dimensions, period and materials

Painting	Dimensions	Age	Materials and artistic technique
<p>1 <i>Madonna con Bambino</i> <i>Madonna with Child</i></p> 	530 × 900 × 14 mm	Fifteenth century	<p>Wood species: Poplar Number of boards and orientation: two vertical tangential (approximately 40 mm from the pith), respectively 275 mm and 255 mm wide Preparation and painting technique: thick gesso and animal glue preparation with the use of canvas; egg tempera paints</p>
<p>2 <i>S. Lodovico e S. Giuliano</i> <i>Saint Lodovico and Saint Giuliano</i></p> 	67 × 1310 × 33 mm	Fifteenth century	<p>Wood species: Poplar Number of boards and orientation: three vertical radial boards (approximately 20 mm from the pith), respectively 170 mm, 380 mm, and 145 mm Preparation and painting technique: thick gesso and animal glue preparation with the use of canvas; egg tempera paints</p>
<p>3 <i>Santa Domenicana</i> <i>Dominican Saint</i></p> 	700 × 1370 × 25 mm	Fifteenth century	<p>Wood species: Poplar Number of boards and orientation: four vertical boards; the first looking from the back is tangential (50 mm from the pith) and 185mm wide; the other three are radial (approximately 20 mm from the pith) and, respectively 165 mm, 130 mm e 220 mm wide Preparation and painting technique: thick gesso and animal glue preparation with canvas; tempera paints and gold leaf Previous conservation treatment: application of a waterproof coating (60% bee wax, 30% paraffine, 10% colophon) on the back face</p>

Table 1 (continued)

Painting	Dimensions	Age	Materials and artistic technique
4 <i>Madonna con Bambino, S. Giovannino e Monaco</i> <i>Madonna with Child, Saint John and monk</i> <i>Madonna with Child, Saint John and monk</i> 	645 × 775 × 23 mm	sixteenth century	Wood species: Poplar Number of boards and orientation: two vertical tangential boards, 210 mm and 435 mm (20 mm from the pith) wide Preparation and painting technique: thick gesso and animal glue preparation; thick oil paints
5 <i>Crocifissione con Madonna e S. Giovanni apostolo</i> <i>Crucifixion with Madonna and Saint John</i> <i>Crucifixion with Madonna and Saint John</i> 	655 × 855 × 30 mm	Sixteenth century	Wood species: Poplar Number of boards and orientation: two vertical tangential (approximately 50 mm from the pith) poplar wood boards, 295 mm and 360 mm wide Preparation and painting technique: thin gesso and animal glue preparation; rose primer; thin oil paints
6 <i>Madonna con Bambino</i> <i>Madonna with Child</i> <i>Madonna with Child</i> 	650 × 890 × 28 mm	Sixteenth century	Wood species: Poplar Number of boards and orientation: three vertical boards; the first looking from the back is radial and 225 mm wide; the other two are tangential (approximately 60 mm from the pith) and 320 and 105 mm wide, respectively Preparation and painting technique: thin gesso and animal glue preparation; thin oil paints

mitigated by the insulated panels. RH was controlled using a Preservatech miniOne humidity generator. Ventilation was guaranteed by 6 fans together with the typical functioning of the humidity machine. The temperature and the relative humidity inside the box were measured by an Onset Hobo U12-013 (accuracy ± 0.35 °C and ± 2.5 %) and logged every 15 min. A remote-control system was also implemented; two CEAM LoRa-C Smart digital sensors were installed in the experimentation area, one inside the box and one outside, and connected to T/RH probes (accuracy ± 2 % and ± 0.5 °C), with a sampling interval of 15 min. The data were continuously collected

through the CEAM CWS software, an integrated platform for supervision, monitoring and shared management based on the web-cloud-IoT technology.

Preparatory conditions of panel paintings and RH cycles

Since the aim of the research is to observe the deformational behaviour of the WPPs, the artworks were tested free from their restraining systems. The restraining system was removed to measure the complete deformation of each panel painting, otherwise such deformation is contained by the restraint system. This allowed (a)

Table 2 Schematic diagram of the most relevant geometrical parameters of the DK

Geometry of the DKs			
Painting	e [mm]	m [mm]	z [mm]
WPP1	174	114	12
WPP2	171	114	12
WPP3	173	92	15
WPP4	168	92	15
WPP5	173	114	12
WPP6	167	92	15

The convention concerning positive (front face convex) and negative (front face concave) values of the cupping angle is also shown. Key to symbols; e: distance between the axes of the two columns, where they intersect the back face of the panel (variable in time); m: distance between the centres of the ball joints of the two transducers on the same column (constant, determined by construction); z: distance between the centre of the ball joint of the lower transducer and the back face of the panel along the axis of the column (constant, determined by construction) [28]

comparison of the experimental results and (b) exclusion of nonlinear behaviour, such as monolateral contacts and friction, among others, that would not have allowed a clear comprehension of the measurements. Thus, the complete free deformation was observed and measured. WPP2 had a painted frame glued on the front face that could not be removed. However, it did not affect the tests, because the frame is considered to be a structural feature of the artwork, typical of a precise historical period and

Table 3 Average values of RH and T for each cycle, calculated starting within 3 h from the RH change applied until the next change and their standard deviations

Test name	Average ΔRH [%]	Sd RH [%]	Average T [°C]	Sd T [°C]
ADS 1 Not water-proofed	52–61	±0.2	25.5	±1.0
ADS 2 Not water-proofed	51–60	±0.1	20.7	±1.1
ADS 3 Waterproofed	53–60	±0.1	20.6	±0.4
DES 1 Not water-proofed	62–52	±0.4	25.4	±0.5
DES 2 Not water-proofed	61–56	±0.2	24.8	±1.1
DES 3 Not water-proofed	56–51	±0.3	23.5	±1.0
DES 4 Waterproofed	60–53	±0.3	20.7	±0.5

useful for characterisation of such objects. Inside the box, a rack was prepared to house the WPPs in a vertical position, the contact areas at the bottom were covered by stripes of PTFE to minimise the friction, and on the top,

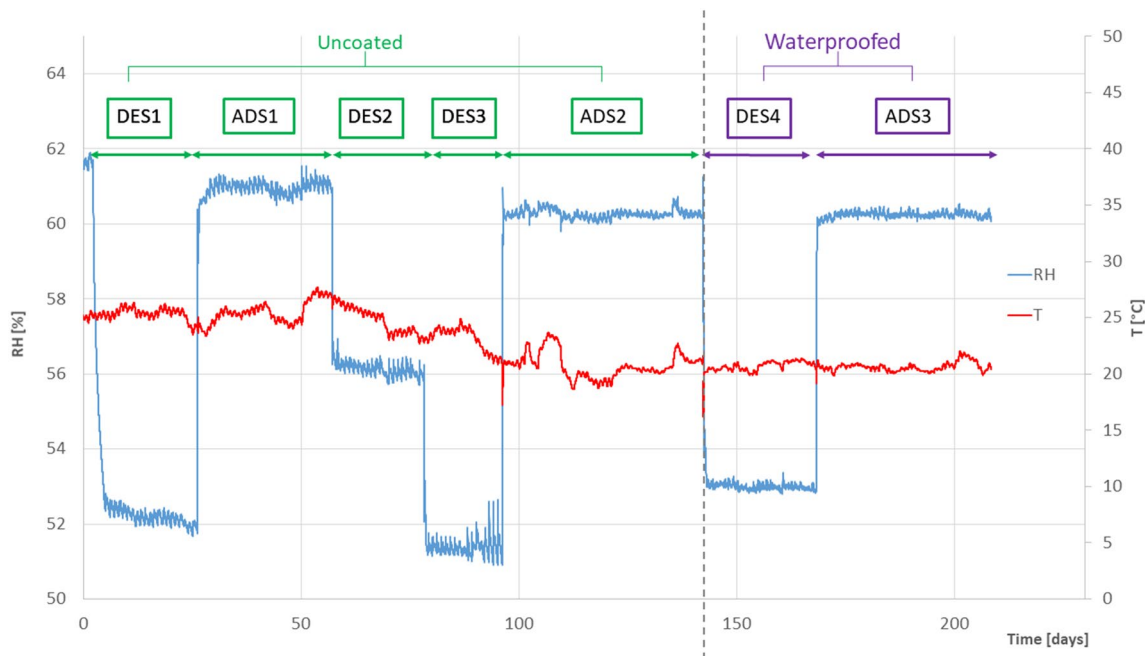


Fig. 1 Relative humidity (RH) cycles for all of the tests performed. The labels indicate the tests, and waterproofing/no waterproofing is reported. In addition, the temperature (T) was reported

a fork covered by foam was fastened on the rack to keep the panel vertical. Prior to the tests, the panel paintings were kept inside the box at 52% RH for 20 days to reach the equilibrium state to avoid moisture gradients.

Together with the restorers and conservators, the climatic range was set between 50 and 65 % RH for the objects' safety and to be representative of their typical conservation conditions. The RH variations were determined by applying the standard EN 15,757:2010 [27] and the concept of historical climate that it introduces. Thus, the conservation climatic conditions were analysed, and the maximum variation of 10 % RH in the range between 50 and 65% was considered safe, in agreement with conservators.

Seven tests were carried out, three in the adsorption mode and four in the desorption mode. The climatic conditions of the tests are described in Fig. 1 and in Table 3.

The procedure of the tests (hereafter called ADS#/DES#) consisted of equilibrating the panel paintings to a specific RH value and then changing the settings on the humidity generator to produce the desired Δ RH (the complete cycles of RH variations imposed are reported in Fig. 1). The new equilibrium condition was considered to be reached when the deformation became flat and stable. During each test, the derivative of the deflection curves was determined repeatedly. Once the derivative is calculated to be zero for at least 6 h, the WPP was considered to be equilibrated to the new RH conditions.

Two of the RH cycles imposed on the paintings, namely, DES4 and ADS3, were performed with waterproof protection applied on the painted face. This is done to evaluate the hygroscopic behaviour of the WPPs when the influence of the emissivity of the front face is nullified and one of the three variables assumed by the study is excluded. Prior to applying the aluminium foil for waterproofing, the four edges of the panel paintings were prepared with Japanese paper glued on the four edges with animal glue, on which the foil was fastened. The choice to protect the edges of the wooden panel by placing Japanese paper made the operation safe and reversible. Then, the painted face was covered by aluminium foil and sealed by silicone tape on Japanese paper. The aluminium foil is impervious to water vapour [29] and much less stiff than wood, with a much lower thickness than that of the wooden supports. In addition, the aluminium foil was chosen to be larger than the artworks to avoid tensions on the painted face.

Since the analysed RH cycles vary in different quantities, the data are normalised to the 5 % RH variation; that is, the deflection was scaled to a 5 % variation in RH. The normalisation is based on the assumptions that the isotherm was explored within its linear part from 51 to 62 % RH, where the behaviour is completely reversible,

and the plastic phenomena excluded. The viscoelasticity was considered to be a linear phenomenon as well. In addition, to enable comparison of the results for the six WPPs, the data are normalised for the span of the DKs. For both cases, the data were divided by a constant (the initial span of the specific DK or the RH variation) and multiplied by a) 5 to normalise for the RH, which is the minimum hygroscopic variation (Fig. 1) imposed on the WPPs, and b) 300 to normalise for the span, which is the width arbitrarily chosen for the modelling to avoid edge effects because an average width of 400 mm was arbitrarily chosen (see “numerical modelling” Section).

Numerical modelling

The numerical modelling is applied to assess, through a sensitivity study, the influence and the mutual interactions of the identified dimensioning variables (layers stiffness, moisture diffusion and emissivity, anatomical cut) in determining the deformation of the painted board. It is important to emphasise that the aim of this numerical model is to create an interpretative method to improve the understanding of the experimental results and in particular of the relationships between certain variables in the theoretical physical model.

For the simulation of moisture diffusion in wood, a simplified approach consisting of an isotropic version of Fick's theory that merges the multiple diffusion mechanisms in wood into a single mechanism [30] was used.

Following [31], the moisture flow is described by.

$$q_m = -\rho_0 \cdot \underline{D} \cdot \nabla m_c \quad (1)$$

where ρ_0 is the wood density in dry conditions, m_c is the moisture content, and \underline{D} is the tensor of the diffusion coefficients that in our case has the following form:

$$\underline{D} = \begin{bmatrix} D_0 \\ D_0 \\ D_0 \end{bmatrix} \quad (2)$$

where D_0 is the value of isotropic moisture diffusion. This approach was already applied by [32, 33] and particularly by [34]. Furthermore, it is theoretically supported by [35, 36], because at room temperature, vapour movement makes only a small contribution to the total transfer movements. This is because bound water movement through the cross walls between cells is two or three times slower than movement across the cell cavity and therefore controls the overall transport rate. Furthermore, [37–39] evidence in the tests carried out using a vacuum sorption balance shows that there are no appreciable differences in the rate of absorption for the specimens in the tangential direction or in the longitudinal

direction. Finally, the time-dependent form of Fick’s law is

$$\frac{\partial m_c}{\partial t} = \nabla \cdot (\underline{D} \cdot \nabla m_c) \tag{3}$$

Assuming it exists, the isotherm of the paint layers is unknown and presumably it varies strongly among the artworks. Similar to [40], we applied the following boundary condition to model its emissivity:

$$\frac{q_t}{\rho_0} = K \cdot (m_{c,air} - m_{c,sur}) \tag{4}$$

where $m_{c,air}$ is the wood equilibrium moisture content corresponding to the air humidity, $m_{c,sur}$ is the moisture content of the wood surface immediately below the ground calculated by the solver, and K is the global effective emissivity of the paint layers. This corresponds to the assumption of perfect adherence between the ground preparation and wood.

First-order hexahedral finite elements were used for the hygroscopic analysis, while second-order hexahedral finite elements were used for the mechanical model.

The applied mechanical model is homogeneous orthotropic linear elastic [41] in cylindrical coordinates with the centre in the pith and considers shrinkage/swelling in cylindrical coordinates. The ground layers were modelled using two-dimensional elements, in accordance with the Kirchhoff–Love theory, that share their nodes with the

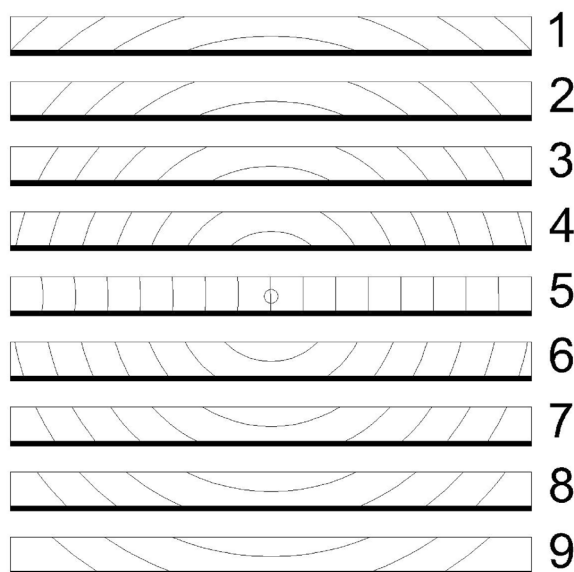


Fig. 2 The geometric model consists of 9 boards typologies virtually obtained by a flat sawn tree trunk. Their dimensions are specified in the drawing. The black area on each board represents the front with the paint layers

Table 4 Mechanical and physical properties of poplar wood used [40, 44]

Young moduli	$E_L = 10,060 \text{ MPa}$	$E_R = 641 \text{ MPa}$	$E_T = 306 \text{ MPa}$
Shear moduli	$G_{RT} = 200 \text{ MPa}$	$G_{TL} = 641 \text{ MPa}$	$G_{LR} = 860 \text{ MPa}$
Shrinkage	$\alpha_L = 0.39\%$	$\alpha_R = 1.92\%$	$\alpha_T = 3.45\%$
Diffusion	$D_0 = 1.52 \cdot 10^{-4} \text{ mm}^2\text{s}^{-1}$		

corresponding nodes of the wood surface. The geometry and discretisation were carried out with the open-source software Salome-Meca developed by EDF (Électricité de France), the simulations with the open-source solver code_aster [42], and the handling of cylindrical coordinates in the solution of the computational model with the open-source software Mfront [43].

The geometric model is made of 9 boards typologies of $400 \times 30 \text{ mm}$, where each board has the same side (front face, the face below in Fig. 2) covered by paint layers and the opposite one (back face, the up face in Fig. 2) free to exchange moisture with the environment. Boards 1–4 represent the common cut for the construction of the WPPs [8], board 5 is a radial cut, and boards 6–9 represent the WPPs ‘painted backwards’ (a panel painting with paint layers on the ‘opposite’ face than the most common cases found in conservation literature). The selected WPPs (Table 1) are associated with the model boards as follows: WPPs 2 and 3 are associated with virtual boards 4 and 5, and WPPs 1, 4, 5 and 6 are associated with virtual board 4. The thickness of the paint layers was chosen as 0.5 mm as an approximate average value among those found in [11]. The boards have a uniform thickness along the longitudinal direction of the wood, with no diffusion phenomenon allowed in this direction; they are also isotatically free to deform. However, the influence of D or thickness is not decisive for the classification of deformation tendencies because their different values manifest the same typological characteristics.

The material properties used for poplar wood reported in Table 4 are based on [40, 44].

Through the numerical model, the deflection of the central span, measuring 300 mm (see “Preparatory conditions of panel paintings and RH cycles” Section), of each of the 9 boards is extracted and plotted over time, drawing a point every 24 h for 60 days.

For these simulations, the following simplifications have been applied:

- (1) All materials are homogeneous, and their characteristics are not moisture-dependent;
- (2) All materials behave purely elastically, and phenomena such as viscoelasticity, mechanosorption and plasticity are not taken into account;

Table 5 Sensitivity study, with indication of paint layer rigidity and emissivity for the 50 cases analysed

Model id	Paint layers rigidity [MPa]	Paint layers emissivity [mm s^{-1}]	Model id	Paint layers rigidity [MPa]	Paint layers emissivity [mm s^{-1}]
1	No rigidity	Bare wood	26	5000	1.00E – 05
2	No rigidity	1.00E – 04	27	5000	7.50E – 06
3	No rigidity	7.50E – 05	28	5000	5.00E – 06
4	No rigidity	5.00E – 05	29	5000	2.50E – 06
5	No rigidity	2.50E – 05	30	5000	insulated
6	No rigidity	1.00E – 05	31	7500	bare wood
7	No rigidity	7.50E – 06	32	7500	1.00E – 04
8	No rigidity	5.00E – 06	33	7500	7.50E – 05
9	No rigidity	2.50E – 06	34	7500	5.00E – 05
10	No rigidity	Insulated	35	7500	2.50E – 05
11	2500	Bare wood	36	7500	1.00E – 05
12	2500	1.00E – 04	37	7500	7.50E – 06
13	2500	7.50E – 05	38	7500	5.00E – 06
14	2500	5.00E – 05	39	7500	2.50E – 06
15	2500	2.50E – 05	40	7500	Insulated
16	2500	1.00E – 05	41	10,000	Bare wood
17	2500	7.50E – 06	42	10,000	1.00E – 04
18	2500	5.00E – 06	43	10,000	7.50E – 05
19	2500	2.50E – 06	44	10,000	5.00E – 05
20	2500	Insulated	45	10,000	2.50E – 05
21	5000	Bare wood	46	10,000	1.00E – 05
22	5000	1.00E – 04	47	10,000	7.50E – 06
23	5000	7.50E – 05	48	10,000	5.00E – 06
24	5000	5.00E – 05	49	10,000	2.50E – 06
25	5000	2.50E – 05	50	10,000	Insulated

- (3) The diffusion along the radial and tangential directions is considered to be the same to reduce the number of significant variables, because for now it is not possible to quantify them experimentally;
- (4) The water vapour resistance of bare wood on the back of painted boards is neglected as it is not known a priori, considering that various products were often applied on the back of the artworks to stabilise its deformational behaviour, in addition to the natural ageing phenomenon of the exposed back;
- (5) At the initial equilibrium conditions, the whole body does not present stresses and strains, and it is planar in the initial conditions;
- (6) Since, due to their physical structure, paint layers have much lower shrinkage and swelling coefficients [14] than wood in transverse directions, the

effect of mechanical hygroexpansion is neglected in the mechanical modelling of paint layers.

A – 1% step variation in the equilibrium moisture content (EMC) is used in the modelling.

To understand the mechanical interaction of the paint layers stiffness with their emissivity, a sensitivity study was carried out by varying their stiffness values, with constant hygromechanical parameters of the wood (Table 4). The sensitivity study is presented in Table 5, where the 50 simulated cases are reported. The table is divided into 5 blocks, each representing a specific rigidity of the paint layers, starting from paint layers hypothetically with zero rigidity arriving to the maximum, which for this work is considered 10^4 MPa, representing the maximum stiffness value identified in [45]. For each block, the paint layer emissivity imposed is also reported.

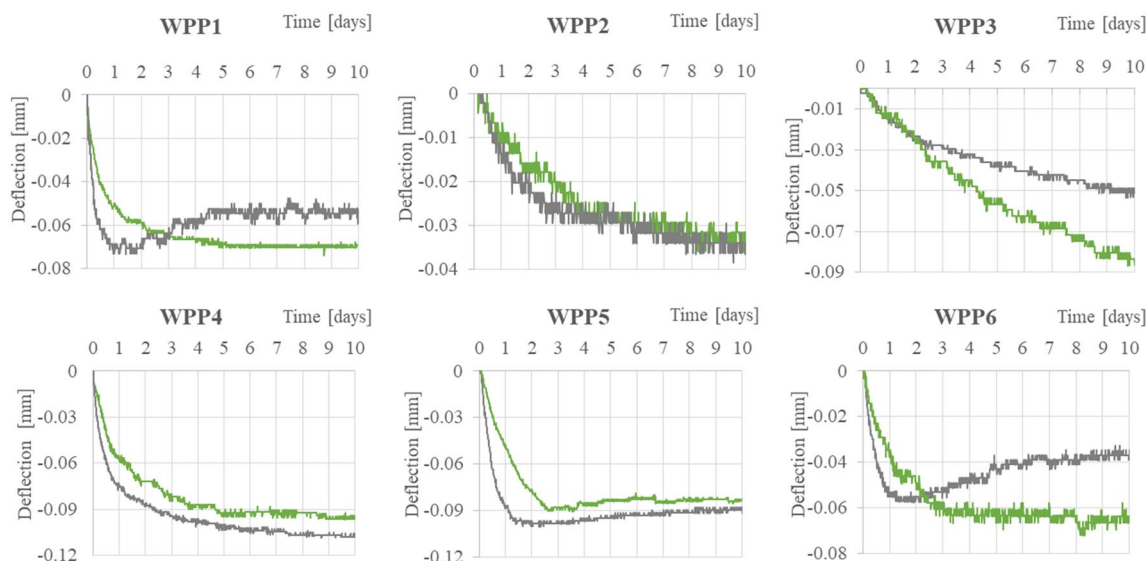


Fig. 3 The hygroscopic deformation behaviour of the 6 panel paintings monitored. The green curves represent the deflection of the WPPs under free exchange of humidity, and the grey curves represent the deflections when the front of the panel is waterproofed by the aluminium foil

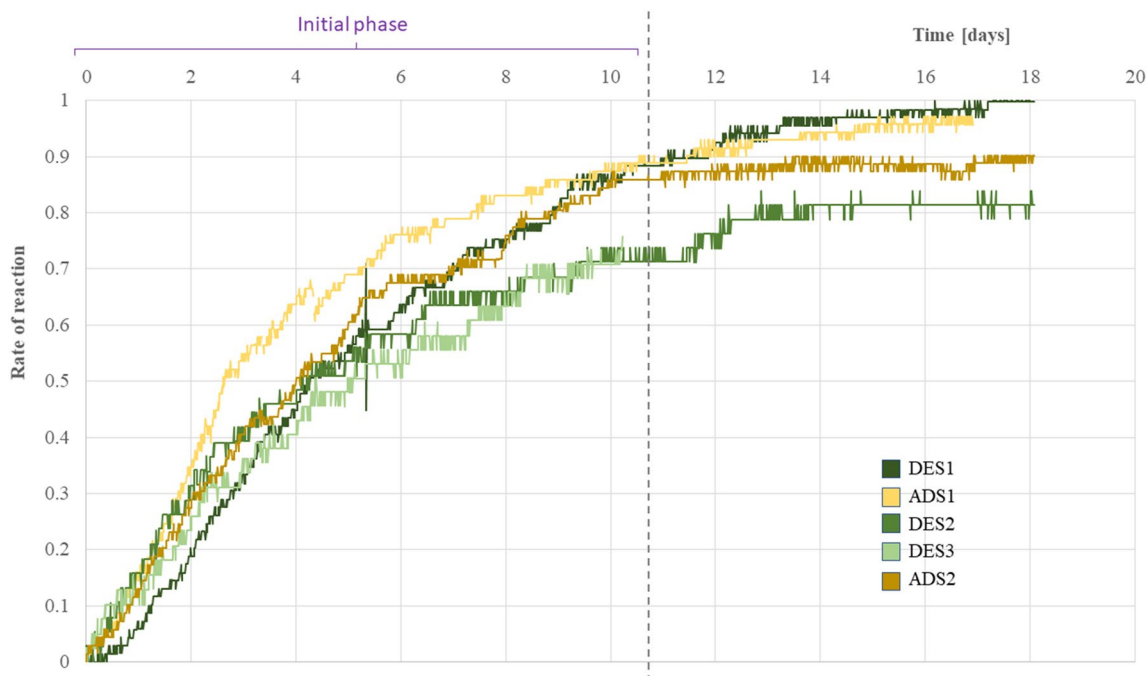


Fig. 4 Representation of the deformational behaviour of WPP3 subjected to different moisture cycles. Each curve represents a different moisture cycle carried out in adsorption (green) or desorption (yellow). All curves show the normalised data and a positive deflection both for adsorption and desorption tests to make the data easier to compare

Results

The experimental results relevant to the RH cycles applied to the six WPPs are presented in graphs and tables in this section. Here, the deformation behaviour

and the quantitative results of the experimental tests are presented separately from the sensitivity study carried out by numerical modelling.

Deformational behaviour and quantitative results

The graphs reported in Fig. 3 show the evolution of the deflection δ [mm] between the two columns of the DKs over time in the group of monitored WPPs. The deflection is calculated as the distance between the midpoint of the (imaginary) line constructed between the bases of the DK columns and its projection normal to the back surface of the painting; therefore, the deflection is calculated in the central 300 mm of the 400 mm virtual table.

The deflection curve of each of the WPPs tested shows two distinct phases (Fig. 3): the initial phase with a very steep change and the second phase where the curve flattens out. This behaviour is typical of any wooden board during a moisture cycle, where the initial faster moisture adsorption or desorption is followed by a weakening of adsorption or desorption rate when the new equilibrium is approaching. The curves in Fig. 4 refer to the rate of reaction of WPP3 during the different cycles carried out in both adsorption and desorption modes. The rate of reaction was calculated by dividing the deflection data by the average deflection at the equilibrium of test DES1 that produced the greatest deflection for WPP3. Figure 4 shows the clear presence of hysteresis in the deformation panels that is caused by the different equilibrium moisture content that the wood exhibits depending on whether it is in the adsorption or desorption phase. However, these differences appear to make a negligible contribution to the qualitative and quantitative amount of deformation.

In all examined paintings (Fig. 3), the first phase is typically concluded within the first 9 days, a time during which the moisture gradients triggered by the different emissivities of the two surfaces of the WPP play a significant role in driving the panel deformation. The deformation at the new equilibrium is the result of the interaction between the anatomy (i.e., growth ring arrangement) of the wooden board and the stiffening caused by the presence of the paint layers. Among the WPPs (Fig. 3, green curves), only WPP5 shows the so-called 'flying wood' (FW): the typical deformational behaviour induced in the presence of a significant hygroscopic and/or mechanical asymmetry of the two opposite faces in a wooden panel. Although hygroscopic and mechanical asymmetry is certainly present to the same extent in all the other paintings, their deformation curve does not show FW behaviour. This experimental evidence appears to suggest that in addition to hygroscopic asymmetry, flying wood deformation can also be generated by the effect of other variables and of their combinations that influence the deformational behaviour of the WPPs.

To assess the existence and the possible influence of a moisture emissivity of the paint layers, the same RH cycles were repeated modifying the hygroscopic

behaviour of the painted surface, with the introduction of the waterproofed barrier that increased the hygroscopic asymmetry between the two surfaces of each WPP (this facilitates the build-up of steep moisture gradients and, as a consequence, the possible occurrence of transient deformations of flying wood [46]). The results obtained show in general a different deformation behaviour of the WPPs, with a new set of deflection curves over time. These curves (grey lines in Fig. 3) differ in both shape and rate of deflection from those shown by the same panel in the nonwatertight mode, with a certain variability among the panels with the same constraint conditions and between the same artwork with different constraint conditions.

For almost all WPPs, the very initial segment of the two curves is characterised by an overlapping of the two phases (this is particularly clear in WPP3, where the treatment applied on the back prolongs this stage). In this initial stage, the paint layers, even in free conditions, exert an effective barrier to moisture diffusion; the point at which the two curves separate can be interpreted as an indication of the specific emissivity to moisture diffusion of each singular WPP.

WPP2 did not show any significant variation between the two cycles. This behaviour can be explained considering the stiffening effect caused by the presence of the wooden cusp frame at the front of the painting.

In all other WPPs, the waterproofed deformation curves are steeper than those with no-waterproofing barriers (typical condition of the panel paintings), highlighting the potential importance of gradients (that are certainly higher in the first case) on the transient behaviour of panel deformation.

However, the most interesting aspects are represented by the difference in the amounts of deformation between the two cycles at the new equilibrium, as shown by WPPs 1, 3, and 6 (WPPs 1 and 3 are both characterised by a

Table 6 Quantitative deformational behaviours of the non-waterproofed WPPs studied

	δ_{\max} [mm]	Time to reach δ_{\max} [days]	Time to reach equilibrium [days]
WPP1	-0.074 ± 0.003	8	8
WPP2	-0.030 ± 0.003	9	9
WPP3	-0.087 ± 0.003	9.5	9.5
WPP4	-0.209 ± 0.003	6	6
WPP5	-0.094 ± 0.003	3.5	6.5
WPP6	-0.067 ± 0.003	5.5	5.5

Note that the time to reach the maximum deflection and the time to reach equilibrium are the same for all WPPs except for WPP5, which is the only one to show FW behaviour

thin support and thick ground layers). If the deformation depends only on the anatomical cutting of the wooden board, in the steady state, the curves in the two test conditions should converge to almost the same values as those in WPPs 4 and 5, where the differences are less evident. This different behaviour suggests a nonlinear moisture-dependent behaviour of the paint layers, whereas a cause related to the hysteretic behaviour of the wood appears to be ruled out, considering that this differentiation does not occur in the other paintings and that both cycles were carried out in desorption mode. Thus, it appears that the stiffness of the paint layers may influence the anatomical behaviour of the wooden panel, allowing the hypothesis that the interaction of paint layers with moisture may change both its mechanical properties and behaviours (in uncovered conditions, the painted layers appear to be less stiff).

With the front face waterproofed, WPP5 confirmed the same FW behaviour that was also observed in WPP1 and WPP6 in this hygroscopic cycle. This observation is a clear demonstration that in some cases, the paint layers exhibit an emissivity that does not allow the formation of a significant gradient between the two faces of the panel. By contrast, when the emissivity is artificially increased, the formation of a strong hygroscopic asymmetry leads to FW behaviour, as theoretically expected. On the other hand, WPP3 and WPP4 maintained the same nonflying wood behaviour observed in the non-waterproofed tests, even when hygroscopic asymmetry was induced. In WPP 4, the thick gesso layer and the thick oil pigments almost completely insulated moisture diffusion, and the paint layer behaved in almost the same manner in both free and waterproofed conditions.

The quantitative aspects of the abovementioned observations are reported in Table 6, where for each WPP, the maximum deflection (δ_{\max}), the time that occurred to reach it and the time to reach equilibrium are presented.

Sensitivity study on the six studied panel paintings

The influence and the mutual interactions of the variables assumed to be the most important on the deformation behaviour of WPPs can be better understood through the sensitivity analysis carried out by

numerical modelling (see “numerical modelling” Section). The main results of this study are presented in Fig. 5.

Here, each diagram represents a hygro-mechanical transient simulation in terms of maximum deflection (δ_{\max}) for boards 1–5 (Fig. 2). Boards 6–9 were omitted from this study because they are a very rare occurrence in WPPs. Each single row of Fig. 5 can be interpreted as the effect produced on the deformational behaviour by the progressive reduction in the emissivity of the paint layers (i.e., cases 1 and 5 will degenerate into 10, cases 11 and 15 into 20 and so on). The column relative to the lowest emissivity can be considered to be a direct estimate of the stiffness of the paint layers; notably, the waterproofed panel paintings with stiff layers will not show flying wood, unlike panel paintings with less stiff layers.

Note that some of the situations represented in Fig. 5 are well described in wood science:

1. Graph 1 is simply the case of boards desorbing equally from both sides with unstiffened surfaces (hygroscopic and mechanical symmetry);
2. Graph 10 shows the case of a board free to exchange moisture on one side only, and the opposite face is completely waterproofed (maximum hygroscopic asymmetry);
3. Graph 41 shows the case of boards free to exchange moisture on both sides and strongly stiffened on one face only (maximum mechanical asymmetry).

The models provide evidence for the presence of five macrocategories, as shown in Fig. 6, characterised by:

- a. Non-Flying wood behaviour with an asymptotic concave deformation relative to the painted face, typical of WPPs ‘painted backwards’ and with paint layers with low stiffness;
- b. Flying wood behaviour without residual concavity relative to WPPs painted on a radial board with low-to-high stiffness of the paint layers;
- c. Non-Flying wood behaviour with convex asymptotic deformation relative to the painted face, typical of

(See figure on next page.)

Fig. 5 Results from the sensitivity study. The numbers represent the model ID of the analyses of Table 5; for simplicity, 15 cases among 50 were chosen, and the deflection [mm] versus time [days] is shown in the graphs, when a hypothetical decrease in RH corresponding to a 1% moisture content occurs. The graphs are sorted according to both paint layer rigidity (mainly of the ground layers) and emissivity. The latter increases from right to left, while the rigidity increases from bottom to top according to the values in Table 5. Case 10 represents the lowest rigidity and the lowest emissivity, while case 41 represents the highest rigidity and the highest emissivity. Moreover, case 1 represents the greatest paint layer emissivity and lowest paint layer rigidity; by contrast, case 50 represents the lowest emissivity and the greatest rigidity. The lower part of the figure shows the geometric reference model for each type of board that was associated with a different colour for each anatomical orientation. The values of the ordinates are proportional to the estimated deformation values to allow a better understanding of the deformation behaviour

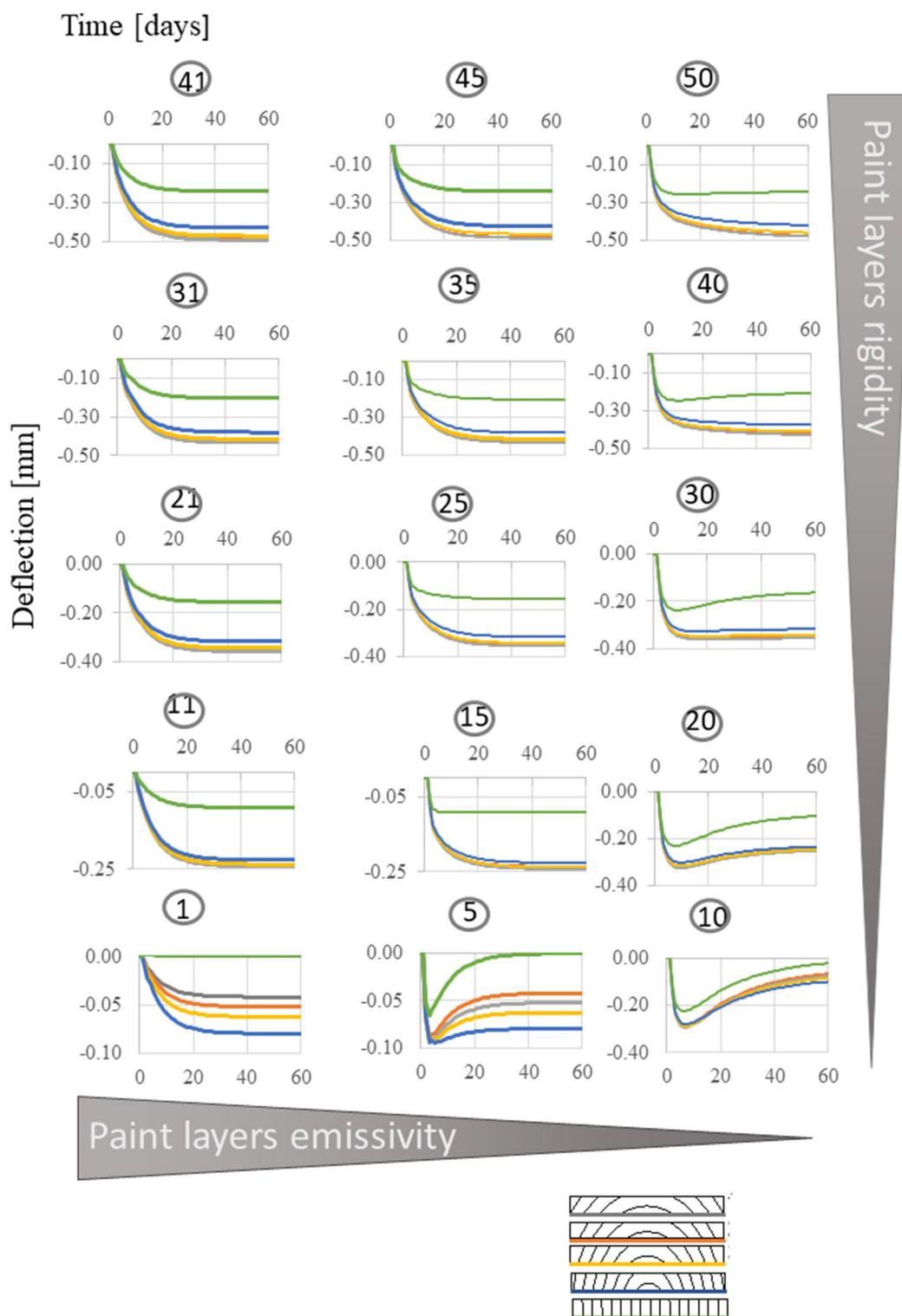


Fig. 5 (See legend on previous page.)

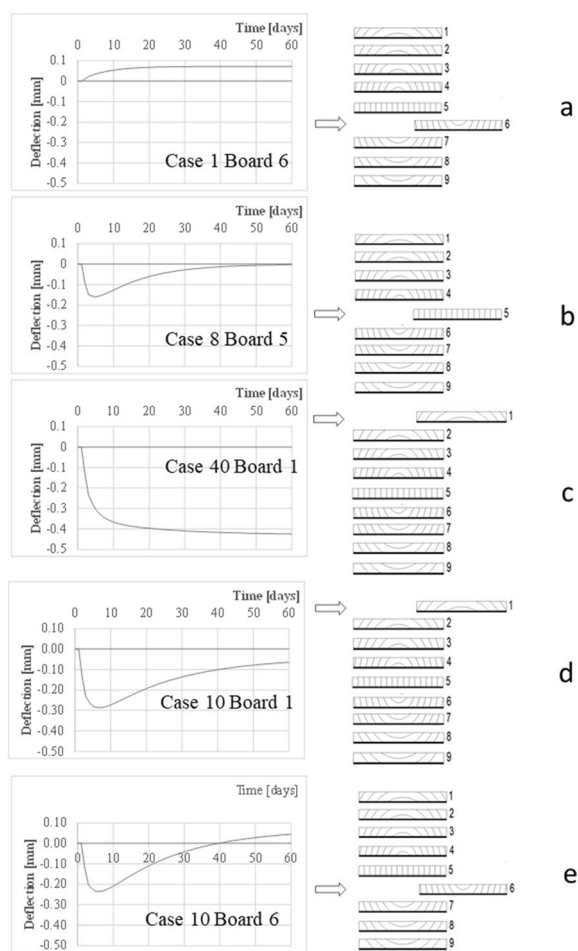


Fig. 6 The macrocategories of the deformation behaviour of the WPPs

- WPPs painted on a tangential board with high stiffness and low emissivity;
- d. Flying-wood-type behaviour with a concave asymptotic deformation relative to the painting face, typical of WPPs 'painted backwards' on a tangential board with low emissivity and stiffness of the paint layers;
- e. Flying wood-type behaviour with convex asymptotic deformation relative to the painting face, typical of WPPs painted on a tangential board with low emissivity and stiffness.

Cases c and d represent the actual effect of the stiffness of the paint layer in a radial board that are cases where the anatomical component of the deformation tendency is absent.

It is observed that the FW and non-FW behaviours can be associated to the extreme (low and high) values of both stiffness and emissivity but also that they can coexist with the same stiffness and emissivity of the paint layers

but with hypothetical different anatomical cutting of the boards (e.g., cases 30, 40, and 50 in Fig. 5 and Fig. 7). This suggests that the three parameters, namely emissivity, stiffness, and anatomy of the wooden board, either acting by themselves or coupled with each other, identify a conceptual domain of panel deformation, within which the actual deformation behaviour of a specific panel painting may occur.

Despite the simplifications introduced in the model, the deformation modes derived from the model application demonstrate a variability and a high degree of complexity of the phenomenon studied to strongly question whether it is truly possible to determine a priori the deformation tendencies of an individual WPP in the absence of a specific characterisation.

Aggregating all of the patterns of Fig. 7, it is possible to determine the existence domain of deformation of a WPP when wood species and panel thickness are given (Fig. 8).

Although the simulation reported in Fig. 8 represents a simplified condition with a constant board thickness of 30 mm, it suggests that the effect of the three variables considered and their reciprocal interactions can produce a hypothetical field of variation, here labelled the 'existence domain', that is highly articulated and has been confirmed by the experimental observations. This consideration introduces the possibility of considering the WPPs as a complex system that shows evolutionary—materials modification with time—and nonlinear behaviours.

Discussion

The analysis performed directly on the experimental data (Fig. 3), leads to the following observations:

- Most of the WPPs studied under normal conditions, without waterproofing foils, show nonflying wood behaviour, and only WPP5 shows FW behaviour in every test condition. This suggests that the combination of the main considered variables (i.e., emissivity and stiffness of paint layers) does not produce the same deformation behaviours even among panel paintings with similar constructive typologies (see WPP5, WPP6) and anatomical cuts (all paintings studied are assimilable to the cutting typology number 4 of Fig. 2).
- Each painting behaves differently if tested with the painted surface free to exchange humidity with the environment or in waterproofed condition. This indicates a nonnegligible moisture transfer through the ground and the paint layers that plays a significant role as a driver of deformation for the wooden support.

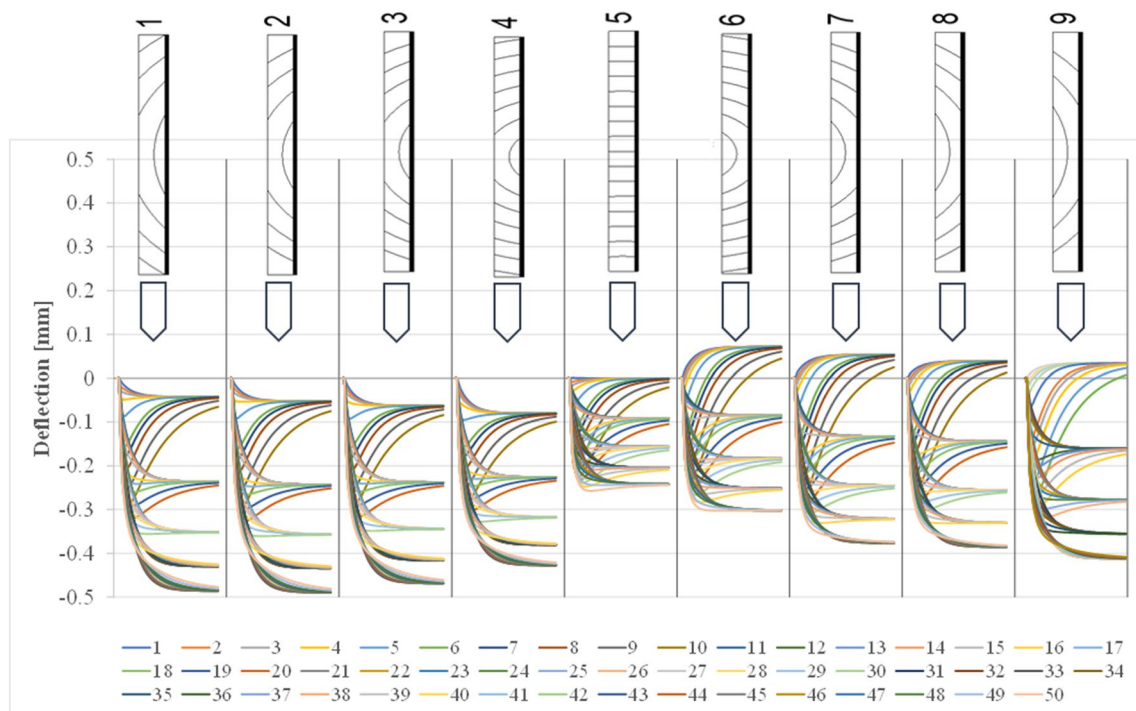


Fig. 7 Deformation tendency of wooden panel paintings examined by anatomical cut, depending on paint layer emissivity and ground layer rigidity. Each family of curves represents the 50 calculated models (Table 5) for each different cut of the table: this shows the enormous variability of values that can occur both within the same table and between different tables. It is emphasised that within the same table, variations in the stiffness of the paint layers and their emissivity alone can reduce the deformation tendency by up to an order of magnitude

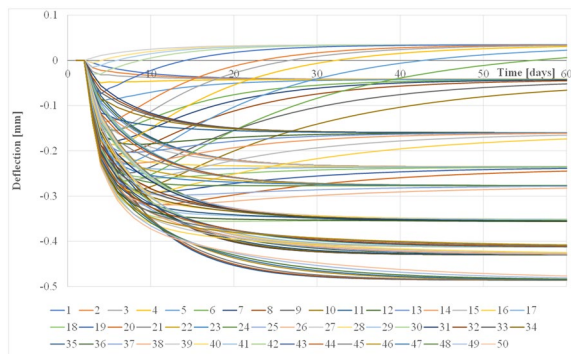


Fig. 8 The existence domain of the deformation of a WPP with a thickness of 30 mm and properties reported in Table 4, according to variations in the anatomical cutting of the board, the paint layer emissivity and the ground layer rigidity

- The face waterproofing led some paintings to assume FW behaviour, which does not occur under normal conditions. In the performed tests, all of the variables remained the same except for the induced hygroscopic asymmetry (only the back was allowed to exchange humidity), and it can be deduced that the internal moisture gradient has a critical influence

on panel behaviour. As stated in [24], the rigidity of the ground layers can cause a lack of FW behaviour. However, the presented numerical modelling and experimental results clearly demonstrate the necessity to couple the rigidity and the emissivity of the paint layers. Based on the experimental results produced in the present work, the generalised stiffness of the preparation (intended as the stiffness of the material and its thickness) and its water vapour emissivity appear to be two strongly coupled and interdependent variables in determining the actual deformation tendencies in a specific WPP.

- A third ancillary observation is that all paintings, chosen a priori by conservators as representative of different historical typologies, behave differently in terms of deformation tendencies, either with a free-to-exchange front or with its total insulation.

The experimental observation allowed us to establish three main families of behaviour:

1. Panel paintings that do not present flying wood in both configurations (WPP3, WPP4);

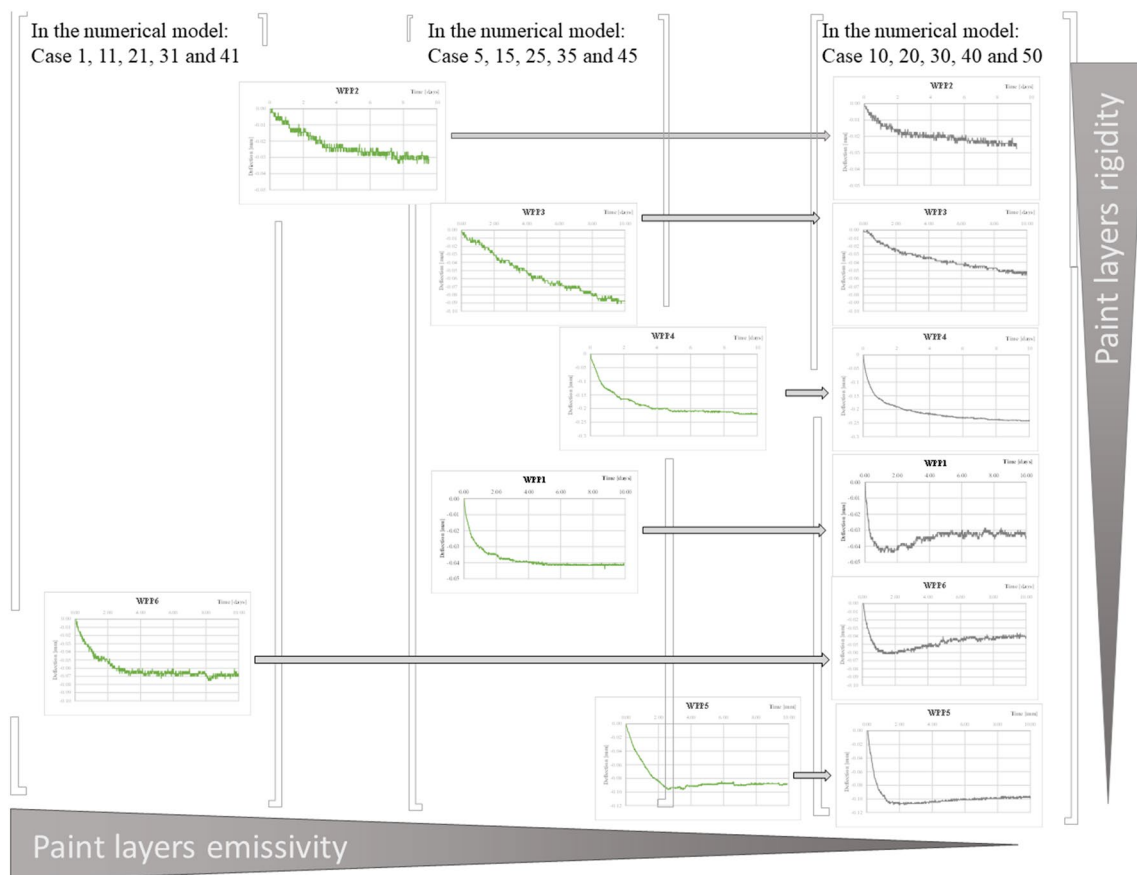


Fig. 9 Experimental results are qualitatively placed in a graph similar to Fig. 5. The waterproofing of the paint layers allows us to reduce the problem of their emissivity variable and leads us to identify its level of stiffness and its deformation consequences. This is realised in the row of diagrams in the last column on the right. The location of the WPPs is approximate

2. Panel paintings that do not have FW behaviour under normal conditions but do show FW behaviour with the waterproofing of the painted face (WPP1 and WPP6);
3. Panel paintings with flying wood in both configurations (WPP5).

Overlapping the results of the sensitivity study with those obtained from experimental observations for real cases allows us to collocate the studied paintings within the existence domain identified by the modelling.

In Fig. 9, a correlation between the WPP behaviours and the diagrams of Fig. 3 is shown. The approximate location of each painting and its deformation state transition due to the waterproofing of the paint surface are shown on a paint layer rigidity/emissivity diagram.

As a result, the three previously identified families can be related to decreasing values of the stiffness of the paint layers relative to the stiffness of the wooden support.

In Fig. 9, it is clearly observed that the application of the aluminium foil makes the paintings comparable in terms of their general deformation mode, bringing them into the vertical zero-emissivity zone on the right part of the diagram. Thus, overall, 3 panel paintings express a low stiffness of the paint layers, and the other 3 show a pronounced stiffness to prevent flying wood due to the strongest possible asymmetry of the internal moisture gradient. The deformation mode of WPP 4 is dominated by the stiffness of the ground layer, while in WPPs 1 and 6, the low stiffness of the paint layers makes the emissivity of the ground layer the dominant driver of the deformation tendency. Finally, experiments show that the case

of WPP 5 represents the limiting case of low emissivity and low stiffness of the paint layers.

Conclusions

The present experimentally examined WPPs matched with comparative results obtained by numerical modelling and applied to understand and characterise their deformation behaviour.

Experimental analysis of a significant sample of WPPs subjected to environmental hygrometric variations revealed the complexity of these objects and a high level of variability in terms of materials and deformation behaviours.

Once the species and thickness of the wood panel were established, three variables were identified as determining factors: the emissivity and stiffness of the paint layers and the cut of the panel in relation to the pith of the tree (anatomy). Each of these factors independently can determine not only the extent of maximum deformation of the paintings but also the deformation behaviour. Therefore, the obtained results suggest that in the presence of hygroscopic variations, these factors are strongly coupled in determining the WPP deformation.

Moreover, the waterproofing of the paint layers demonstrated that (i) the front layers show a nonnegligible flow of humidity; (ii) it is possible to evaluate the deformative effect of the stiffness of the paint layers (iii) as well as the actual effect of the emissivity of paint layers on the global deformation behaviour of the panel; and (iv) it is possible to identify deformation families. For conservation, the deformation tendency of the panel determines the choice and sizing of any restraining system, such as crossbeams and frames, and, together with reactivity, the design of any climatic control system. Its nature as a complex system, as appears from this study, underlines the necessity to consider every panel as unique object, the state of which needs to be characterised prior to the implementation of any conservation treatment or preventive conservation and climate control plan. Each WPP is also a complex and unique system affected by nonlinear state-dependent behaviour. Each of the parameters characterising these artworks (layers hygroscopicity, mechanical stiffness, anatomical cutting, and conservation environments) constitute a set of interconnected and interacting physical subsystems, whose temporal evolution (the rules by which they evolve over time), which is not random, is highly dependent on knowledge of the initial conditions, boundary conditions and inner structural mechanics characterisation. Since a small difference in these conditions can lead to very different characteristics and behaviour of the system, as any other state-dependent nonlinear system, WPP may not be predictable even if the variables and equations governing them are known. Therefore, for this artefacts, deterministic models based on the

use of generic material characteristics and/or on the results of accelerated ageing cycles could yield very modest, if not misleading, results in the interpretation of the behaviour of systems and particularly in the prediction of the evolutionary behaviour of individual artworks. Similar to other complex systems, in the case of WPP, their behaviour cannot be predicted but only measured. By contrast, if all material properties and boundary conditions are specifically determined through direct experimentation on real works of art—as in the methodology introduced in this work—then results of the numerical simulations can be accurate and correspond to the actual behaviour of the artworks. In any case, numerical simulations are useful for classifying real objects and explaining observed phenomena; this means that numerical methods should be used to extend the knowledge provided by experimental results.

Acknowledgements

Not applicable.

Author contributions

Lorenzo Riparbelli designed the tests, discussed the results, developed and discussed the numerical model, analysed and discussed the physics of the panel paintings, wrote and revised the paper. PM. designed the tests, processed and discussed the experimental data, participated in discussing the model results, wrote and revised the paper. CM. Processed the data, prepared Tables 1, 2, 3, 4, 5, 6 and Fig. 1, revised the paper. LU. Designed the tests and revised the paper. GG. Observed and described the six panel paintings. Luciano Ricciardi, SR, AS. and CC chose and provide the six historical panel paintings, participated in designing the tests and revised the paper MF. Participated in designing the tests, discussed the experimental data and the numerical model results, wrote and revised the paper, coordinator of the project. All authors read and approved the final manuscript.

Funding

PREMUDE Project—Tuscany Region—POR-FSE 2014–2020. Modelli innovativi per la conservazione PREventiva in ambienti MUseali e DEpositi temporanei post-emergenza.

Availability of data and materials

The datasets generated and analysed during the current study are available from the corresponding author on reasonable request.

Declarations

Competing interests

Absence of any conflict of interest.

Received: 8 July 2022 Accepted: 4 December 2022

Published online: 06 February 2023

References

1. Buck RD. Some applications of mechanics to the treatment of panel paintings, in recent advances in conservation, international Institute for the conservation of historic and artistic works (IIC), London: G. Thomson, 1963; 156–162.
2. Buck RD. Some applications of rheology to the treatment of panel paintings. *Stud Conserv.* 1972;17(1):1–11.
3. The structural conservation of panel paintings proceedings of a symposium at the J. Paul Getty Museum 24–28 April 1995. Dardes K. and Rothe A. (Eds.). The Getty Conservation Institute. Los Angeles. 1998. ISBN 0-89236-384-3.

4. Facing the challenges of panel paintings conservation: trends, treatments, ad trainings. proceedings of the symposium 17–18 May 2009. Phenix A. and Chui SA. (eds). The Getty conservation institute, US 2011. ISBN 978-0-9834922-2.1.
5. Wood science for conservation COST Action IE0601. Supplement of Journal of Cultural Heritage. <https://doi.org/10.1016/j.culher.2012.06.001>.
6. Uzielli L. Historical overview of panel-making techniques in central Italy, in proceedings of a symposium at the J, Paul Getty Museum 24–28 1995. The Getty Conservation Institute, US1998. 110–135.
7. Wadum J. Historical overview of panel-making techniques in northern countries, in Proceedings of a Symposium at the J, Paul Getty Museum 24–28 April 1995, The Getty Conservation Institute, US 1998; 149–177.
8. Structural conservation of Panel paintings at the Opificio delle Pietre Dure in Florence: method, theory, and practice. Ciatti M, and Frosinini C. (Eds), Edifir. 2016. ISBN 978-887970-792-3.
9. C Cennini, *Il libro dell'arte*, Neri Pozza Frezzato F, 2009. The art book in Italian.
10. Federspiel B. Questions about Medieval Gesso Grounds, in Historical painting techniques, materials, and studio practice: Preprints of a Symposium, University of Leiden, the Netherlands, 26–29 June 1995, The Getty Conservation Institute, US 1995. 58–64.
11. Martin E, Sonoda N, Duval A. Contribution a l'etude des preparations blanches des tableaux italiens sur bois. *Stud Conserv.* 1992;37(2):82–92. <https://doi.org/10.2307/1506400>.
12. Siau JF, Avramidis S. The surface emission coefficient of wood. *Wood Fiber Sci.* 1996;28(2):178–85.
13. P Cremonesi Le vernici finali per i dipinti. *Progetto Restauro*, 2005(29): 16–28. The varnishes for panel paintings. In Italian.
14. Mecklenburg M, Tumosa C, Erhardt D. 1998 Structural response of painted wood surfaces to changes in ambient relative humidity, in *Painted Wood History and Conservation*. The Getty Conservation Institute. Los Angeles. 464–483.
15. Allegretti O, Raffaelli F. Barrier effect to water vapour of early European painting materials on wood panels. *Stud Conserv.* 2008;53(3):187–97. <https://doi.org/10.1179/sic.2008.53.3.187>.
16. De Backer L, Laverge J, Janssens A, de Paepe M. Evaluation of the diffusion coefficient and sorption isotherm of the different layers of early Netherlandish wooden panel paintings. *Wood Sci Technol.* 2018;52(1):149–66.
17. Hendrickx R, Desmarais G, Weder M, Ferreira ESB, Derome D. Moisture uptake and permeability of canvas paintings and their components. *J Cult Herit.* 2016;19:445–53. <https://doi.org/10.1016/j.culher.2015.12.008>.
18. Hoadley B. Chemical and physical properties of wood, in *The structural conservation of panel paintings: proceedings of a symposium at the J. Paul Getty Museum 1995*;24–28.
19. Wood handbook—wood as an engineering material. FPL-USDA, 2010. https://www.fpl.fs.fed.us/documnts/fplgtr/fpl_gtr190.pdf. Last checked 11/01/2023.
20. Mazzanti P, Colmars J, Hunt D, Uzielli L. A hygro-mechanical analysis of poplar wood along the tangential direction by restrained swelling test. *Wood Sci Technol.* 2014;48:673–87. <https://doi.org/10.1007/s00226-014-0633-4>.
21. Hunt D, Uzielli L, Mazzanti P. Strains in gesso on painted wood panels during humidity changes and cupping. *J Cult Herit.* 2017;25:163–9. <https://doi.org/10.1016/j.culher.2016.11.002>.
22. Sassoli M. Characterization of wood aging by means of volatile organic compounds (VOCs) analysis, PhD Thesis, University of Florence. Italy. 2018.
23. Esteban L, Gril J, De Palacios P, Casasa A. Reduction of wood hygroscopicity and associated dimensional response by repeated humidity cycles. *Ann For Sci.* 2005;62(3):275–84. <https://doi.org/10.1051/forest:2005020>.
24. Allegretti O, Bontadi J, Dionisi-Vici P. Climate induced deformation of panel paintings: experimental observations on interaction between paint layers and thin wooden supports, international Conference florence heritech: the future of heritage science and technologies. 949, 2020. <https://doi.org/10.1088/1757-899X/949/1/012018>.
25. Brandao A, Perré P. 1996 “The flying wood”—a quick test to characterise the drying behaviour of tropical woods. In: *Proceedings of the 5th International IUFRO Wood Drying Conference*. Eds Cloutier, A., Fortin, Y., Gosselin, R., Quebec City, Canada. pp. 315–324.
26. Arends T., Pel L., Huinink H.P., Schellen H. L. Dynamic Bending of an Oak board due to a moisture content gradient, poromechanics 2017—proceedings of the 6th biot conference on Poromechanics, 9–13:386–394.
27. EN 15757:2010—conservation of cultural property—specifications for temperature and relative. <https://standards.iteh.ai/catalog/standards/cen/ad03d50b-22dc-4c57-b198-2321863f3870/en-15757-2010>. Last checked 11/01/2023
28. Uzielli L, Cocchi L, Mazzanti P, Togni M, Julien D, Dionisi-Vici P. 2012 The deformometric kit: a method and an apparatus for monitoring the deformation of wooden panels. *J Cult Herit.* 2012;13(3):S94–101.
29. Siau J. Wood influence of moisture on physical properties. Blacksburg: Virginia Polytechnic Institute and State University; 1995.
30. Saft S, Kaliske M. Numerical simulation of the ductile failure of mechanically and moisture loaded wooden structures. *Comput Struct.* 2011;89(23–24):2460–70. <https://doi.org/10.1016/j.compstruc.2011.06.004>.
31. Fortino S, Mirianon F, Toratti T. A 3D moisture-stress FEM analysis for time dependent problems in timber structures. *Mechan Time-Dependent Mater.* 2009;13(4):333–56. <https://doi.org/10.1007/s11043-009-9103-z>.
32. Marcon B, Mazzanti P, Uzielli L, Cocchi L, Dureisseix D, Gril J. Mechanical study of a support system for cupping control of panel paintings combining crossbars and springs. *J Cult Herit.* 2012;13(3):S109–17. <https://doi.org/10.1016/j.culher.2012.04.003>.
33. Marcon B, Goli G, Fioravanti M. Modelling wooden cultural heritage The need to consider each artefact as unique as illustrated by the Cannone violin. *Herit Sci.* 2020;8(1):24. <https://doi.org/10.1186/s40494-020-00368-1>.
34. Rachwał B, Bratasz Ł, Łukomski M, Kozłowski R. Response of wood supports in panel paintings subjected to changing climate conditions. *Strain.* 2012;48(5):366–74. <https://doi.org/10.1111/j.1475-1305.2011.00832.x>.
35. Choong E. Diffusion coefficients of softwoods by steady-state and theoretical methods. *For Prod J.* 1965;15(1):21–7.
36. Skaar C. Wood-water relations. Berlin: Springer-Verlag; 1988.
37. Christensen G, Kelsey K. The rate of sorption of water vapor by wood. *Holz Roh Werkst.* 1959;17:178–88.
38. Christensen G. The rate of sorption of water vapour by wood and pulp. *Appita J.* 1959;13:112–23.
39. Engelund-Thybring E, Zelinka S, Glass S. Kinetics of water vapor sorption in wood cell walls: state of the art and research needs. *Forests.* 2019;10(8):704. <https://doi.org/10.3390/f10080704>.
40. Dureisseix D, Marcon B. A partitioning strategy for the coupled hygromechanical analysis with application to wood structures of cultural heritage. *Int J Numer Meth Eng.* 2011;88(3):228–56.
41. Bodig J, Jayne B.A. Mechanics of wood and wood composites. Van Nostrand Reinhold Publ., New York, USA, 1982.
42. EDF - Électricité De France, Finite element Code_Aster: Analyse des Structures et Thermo-mécanique pour des Etudes et des Recherches. Finite element Code_Aster analysis of the structure and thermo-mechanics to the study and Researches, in French. 2022. <https://code-aster.org/V2/doc/v12/en/index.php?man=R>. Accessed 11 Jan 2023.
43. Helfer T, Michel B, Proix J-M, Salvo M, Sercombe J, Casella M. Introducing the open-source mfront code generator: application to mechanical behaviours and material knowledge management within the PLEIADES fuel element modelling platform. *Comput Math Appl.* 2015;70(5):994–1023. <https://doi.org/10.1016/j.camwa.2015.06.027>.
44. Mazzanti P, Togni M, Uzielli L. Drying shrinkage and mechanical properties of poplar wood (*Populus alba* L) across the grain. *J Cult Herit.* 2012;13(3):85–9.
45. Gauvin C. Etude expérimentale et numérique du comportement hygromécanique d'un panneau de bois : application à la conservation des tableaux peints sur bois du patrimoine, PhD Thesis, LMGC—Laboratoire de Mécanique et Génie Civil, Université de Montpellier 2, France

experimental study and numerical modeling of the hygromechanical behaviour of wood applied to the conservation of panel paintings, in French. 2015.

46. Dionisi-Vici P, Mazzanti P, Uzielli L. Mechanical response of wooden boards subjected to humidity step variations: climatic chamber measurements and fitted mathematical models. *J Cult Herit.* 2006;7(1):37–48.

Publisher's Note

Springer Nature remains neutral with regard to jurisdictional claims in published maps and institutional affiliations.

Submit your manuscript to a SpringerOpen[®] journal and benefit from:

- ▶ Convenient online submission
- ▶ Rigorous peer review
- ▶ Open access: articles freely available online
- ▶ High visibility within the field
- ▶ Retaining the copyright to your article

Submit your next manuscript at ▶ [springeropen.com](https://www.springeropen.com)
